Journal Pre-proof

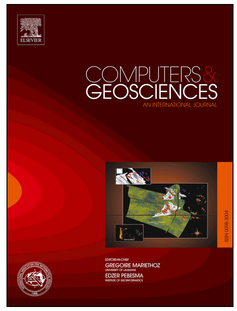

A method and software solution for classifying clast roundness based on the radon transform

G. Moreno Chávez, Jesús Villa, D. Sarocchi, Efrén González-Ramírez

PII: S0098-3004(19)30866-0

DOI: https://doi.org/10.1016/j.cageo.2020.104451

Reference: CAGEO 104451

To appear in: *Computers and Geosciences*

Received Date: 10 September 2019

Revised Date: 11 February 2020

Accepted Date: 18 February 2020

A method and software solution for classifying clast roundness based on the Radon transform

Moreno Chávez G.[a], Jesús Villa [b*], Sarocchi D.[c], and Efrén González-Ramírez[b]

[a] Maestría en Ciencias del Procesamiento de la Información, Universidad Autónoma de Zacatecas, Av. Ramón López Velarde 801, Zacatecas 98000, México.

[b] Unidad Académica de Ingeniería Eléctrica, Universidad Autónoma de Zacatecas, Av. Ramón López Velarde 801, Zacatecas 98000, México.

[c] Instituto de Geología / Fac. de Ingeniería UASLP, Av. Dr. M. Nava No 5, Zona Universitaria 78290, San Luis Potosí, México.

[*]**Corresponding author**. Email address: **jvillah@uaz.edu.mx**

Abstract

In this paper, an algorithm for clast roundness classification based on the Radon transform is presented. The degree of roundness is determined by processing the sinogram of the clast image. The algorithm consists in applying two low-pass filters to the sinogram, obtaining the inverse Radon transform and comparing the filtered images with the original image. For rounded particles, the difference between the original image and either of the filtered images will be small. For angular clasts, the difference will be greater than for rounded clasts, due to the presence of high-frequency components. In the comparison process, each of the two filtered images are subtracted from the original image to yield two difference images. Since the data are binary, these two images present topologically unconnected regions that correspond to the particle's edges. The percentage of non-overlapping area between the original and the difference images, and the number of regions are used to classify the morphology of the clast. The results have been validated using a comparison

Moreno C. G. proposed the method combining image analysis and Radon transform. He developed the algorithm and software. **Villa J.** proposed using the Radon transform to estimate roundness. He contributed to the mathematical framework for the estimation of the Radon transform. **Sarocchi D.** focused on sedimentological aspects and in the application of texture analysis in the geological field. He proposed the experimental framework to test the method. **González R. E.** worked on the estimation of the Gaussian models used in the classification. He also participated in the technique to process the sinogram. All authors contributed to the discussion and conclusions of the manuscript.

chart designed for visual roundness estimation. The comparison chart, consisting of five roundness classes, was proposed by Russell, Taylor and, Pettijohn (Müller, 1967). Two cutoff frequencies, one to classify well-rounded, rounded and sub-rounded clasts and another for angular and sub-angular classes, were used. The proposed algorithm correctly classifies the roundness classes of the visual graph. The results provided by the algorithm were compared with the classification performed by a group of experts. The algorithm assigned 92% of the clasts to the same classes as the human experts. We also propose Gaussian models, which are useful to classify the particles into the five classes. We have developed a user-friendly software to carry out the roundness classification algorithm. This software was developed on the MATLAB platform and can be freely downloaded from the public repository.

Keywords: Clast morphology; roundness; Radon transform; texture analysis

1. Introduction

Clast morphology is a fundamental tool for studies concerning sedimentary textures. Texture analysis of clasts enables information about transport and depositional processes to be inferred. Particle morphology is essential for an accurate study of sedimentary texture, and depends on many variables, such as (1) origin, (2) intrinsic characteristics (hardness, presence of joints, schistosity, among others), (3) particle size, (4) transport and (5) agents of transport (Sneed and Folk, 1958). Complex processes, such as collisions, friction, break-up, transport paths, and dissolution (related to transport, deposition, and erosion), are recorded in the morphology of clasts (Boggs, 2012; Caballero et al., 2012; Folk, 1980; Krumbein and Pettijohn, 1938; Sarocchi et. al., 2008, 2011; Tucker, 2003, 2009).

To define clast morphology is a complex issue, and countless definitions have been given to this term over time (Barrett, 1980; Blott and Pye, 2008; Douglas and Colin, 1993; Krumbein, 1941; Powers, 1982; Winkelmolen, 1982; Zingg, 1935). Barrett (1980) proposed a meaningful definition which has been the base definition for many years. Barrett described the shape of particles by three hierarchical and independent components: form, roundness, and roughness (or surface texture). Form is the major hierarchical characteristic which is related to overall shape. Usually, form is calculated by dimensionless axial ratios. Roundness is an intermediate characteristic and is superimposed on form. The degree of rounding or angularity is related to the curves and main corners. Roughness or texture refers to finer irregularities superimposed on roundness and form (Barrett, 1980; Blott and Pye, 2008; Powers, 1953). These properties are shown in Figure 1.

Figure 1. Form, roundness, and texture as proposed by Barrett (1980)

Various authors have determined the form of clasts quantitatively, generally based on measurements that have to do with the relationship between two or three axes of the particles (Barrett, 1980; Ehrlich and Weinberg, 1970; Krumbein, 1941). This high-order characteristic is well determined. The clasts are measured and classified through simple dimensionless descriptors. In contrast, roundness is a more difficult characteristic to measure. Several mathematical models and algorithms have been proposed over time; they work well but with some limitations (Beddow, 2018). One method is based on measurement of the radius of curvature (Hryciw et al., 2016; Montenegro et al., 2013; Roussillon et al., 2009; Schwarcz and Shane, 1969; Wadell, 1932). Roundness, in this method, is estimated by the ratios of the radii of curvature to that of the circumscribed circle of the perimeter of the clast. An important constraint is that the particle's perimeter must be convex, but the main issue is determining a threshold for the curvature. Another method measures roundness and roughness using a statistical analysis of the distribution of heights (Alshibli and Mustafa, 2004). The surface of the particle is captured by an optical interferometry technique. The mean, median, minimum, maximum, and other parameters are then estimated from the distribution of heights (obtained from the surface) and are used to classify the clast. These methods are accurate but complex because they capture the surface. An outstanding method for morphological analysis is based on Fourier analysis of 2D perimeters (Alshibli and Mustafa, 2004; Caballero et al., 2012; Charpentier et al., 2013; Diepenbroek et al., 1992; Montenegro et al., 2013; Sarocchi et al., 2011). The algorithms provide the Fourier transform of the particle's perimeter and relate bands of harmonics to different aspects of morphology. In general, low frequencies correspond to the particle's form, medium frequencies to roundness and high frequencies to texture. Although this method is accurate, it has the limitation that the perimeter must be convex. Moreover, to assign form, roundness, and roughness to specific frequency ranges is not an easy task (Sarocchi et al., 2011). Fractal geometry is another useful method to characterize a clast's roundness (Kaye, 1978; Orford and Whalley, 1983; Sarocchi et al., 2011). The technique most used to analyze particle boundaries is known as the structured walk. In this technique, irregularities on a particle's perimeter are related to a fractal dimension, which is estimated for 3D clast surfaces by polygons or by line segments for particle perimeter contours. The sides of the polygon are progressively increased. The perimeter calculated from all the sides is plotted on a log-log scale. The fractal dimension 'D' is calculated from the slope of the best-fit line. Some limitations of this method, such as identification of the particle boundary related to the process of abrasion and sensitivity to blur and background noise of the image, are described by Leavers (2000) and Stachowiak (1998).

From a practical and interpretative point of view, it is not enough to measure the degree of roundness but also important to categorize it. A tool used by sedimentologists to classify clast morphology is the visual comparison chart. Russell, Taylor and Pettijohn (Müller, 1967) developed a visual comparison chart of a set of reference particles of known roundness. The chart offers a quick and easy way to semi-quantitatively estimate two-dimensional particle roundness. The Russell, Taylor and Pettijohn (RTP) reference figure has 25 particles organized into five different roundness categories; angular, sub-angular, sub-rounded, rounded and well-rounded (Boggs, 2012).

In this paper, we present a method to classify the roundness of sedimentary rocks based on the Radon transform. For two dimensions, the Radon transform converts the area of the particle into a one-dimensional function which we call a profile. This is achieved through the line integral. The profile corresponds to an angle. The Radon transform maps the area to profiles for all angles $(0°, 180°]$. The result is a two-dimensional function, called a sinogram, whose independent variable is the angle and whose dependent variable is the profile. The sinogram contains useful information to measure or classify the roundness. The algorithm consists in obtaining the Radon transform of the binary image of the class. The resulting sinogram is processed by two filters, one to classify well-rounded, rounded and sub-rounded particles and another for the angular and sub-angular classes. Once the filter is applied, the inverse Radon transform is obtained and the original and filtered image are compared, subtracting the images. Since the images are binary, the difference is a binary image. The percentage difference and number of topologically unconnected regions that correspond to the edges of the particle in the subtraction image are used to classify the clast. The algorithm has been tested using the RTP chart for visual roundness estimation and also compared to a semi-quantitative classification by five experts. Using the percentage difference and number of regions, Gaussian models were proposed to classify clastic particles into five classes. RadonS is a software that we have developed in order to facilitate and extend the use of the proposed algorithm. The RadonS software has a user-friendly graphical interface developed in MATLAB.

2. The Radon Transform

Johann Radon proved that a differentiable n-dimensional function can be determined by hyperplane integrals (Deans, 1983; Helgason, 1999; Radon, 2005). In short, if f is a function defined on a space $\mathbb{R}^2$, the Radon transform of f is determined by the line integrals of f. If (x, y) are coordinates of points in the plane and L is any line in the plane, then the Radon transform is the mapping by line integral of f along all possible lines L,

$$I_R(\rho, \theta) = \Re\{I(x, y)\} = \iint_{-\infty}^{\infty} I(x, y)\delta(xcos\theta + ysin\theta - \rho)dxdy, \qquad \text{Eq.1}$$

where δ represents the Dirac delta function, which rotates the normal vector ρ, and $xcos\theta + ysin\theta$ are the coordinates for integration of the normal line L. As shown in Figure 2, the Radon transform is determined by the integration of all the lines L.

Figure 2. Line L at coordinate (ρ, θ)

Figure 3 shows a graphic example of three line integrals. The result of the Radon transform, composed of line integrals or profiles, is called a sinogram. An example is shown in Figure

4. The sinogram contains all line integrals at all angles. The sinogram has the angle of integration $(0°, 180°]$ on its horizontal axis and the integration on the vertical axis (Deans, 1983; Helgason, 1999).

Figure 3. Example of line integration at three angles: 0°, 45° and 90°.

The Radon transform has been applied to such diverse fields as crystallography, astronomy, microscopy, and remarkably, computed tomography (Kuchment, 2014). Applications to the taxonomy of shape have also been explored (Deans, 1983; Barrett, 1984; Tabbone and Wendling, 2002). The literature on the morphological analysis of particles is scarce. Leavers (2000) carried out one of the few investigations to explore the relationship between morphology and the Radon transform, showing that the Radon transform provides useful information about corners and apexes to describe a particle's shape. The study showed in detail that the Radon transform maps the particle's outlines to a space of bounding curves that express the relationship of each point of the contour with the others. References concerning the study of clast roundness by the Radon transform are not available.

2.1 Roundness classification method

Since the Radon transform is not invariant scaled, the first processing we perform on the image is area normalization to 4500 pixels; this area corresponds to a circle of 205×205 pixels. We chose 4500 pixels because with a general purpose camera 20 objects can be captured (including the space between them). For the three scales proposed by Barrett (1980), twenty clasts represents a good compromise between quality and quantity. Let $I(x, y)$ be the binarized and normalized image of a particle defined on some domain D;

$$I(x, y) = \begin{cases} 1 & x, y \in D \\ 0 & \text{otherwise} \end{cases} \qquad \text{Eq. 3}$$

If $\Re\{\cdot\}$ denotes the Radon transform, then $I_R(\rho, \theta) = \Re\{I(x, y)\}$ represents the Radon transform of an image. As explained above, the Radon transform is a projection defined as a line integral $I(x, y)$ along line L. Because the image processing is discrete, the sinogram of an image is obtained using the discrete Radon transform. For the discrete case, the integral of Eq. 1 is represented by an accumulator (Kelley and Madisetti, 1993) and the set of inclination angles is finite. The algorithm uses integer angles within the range $(0°, 180°]$.

The sinogram resulting from the radon transform has a direct relationship with the contour of the analyzed object. As illustrated in Figure 4, a rounded particle has a blurred sinogram but as the degree of angularity of the rock increases, the blur of the sinogram decreases.

This blurring degree has a close relationship with the frequency components of the clast. For this reason, sinogram processing employing frequency analysis gives useful information to determine the roundness.

Figure 4. Sinograms resulting from the Radon transformation of binary clasts. The particles with different degrees of angularity previously classified by Russell, Taylor and Pettijohn (Müller, 1967).

To separate form and roundness, the sinogram is filtered by a Butterworth low pass filter which is determined by the following expression

$$H(u,v) = \frac{1}{1 + [D(u,v)/D_0]^{2n}} \quad \text{Eq. 5}$$

where n is the order of the filter, D_0 is the distance from the origin to the cutoff frequency, the tuple (u, v) represents the Fourier space, and $D(u,v) = \sqrt{u^2 + v^2}$. Choosing a suitable order and distance, the filtered sinogram $I_f(u,v) = I_R(u,v)H(u,v)$ will contain only the general form. As can be seen, filtering is carried out in the frequency domain, so $I_R(u,v) = \mathcal{F}\{I_f(\rho,\theta)\}$ and $I_f(\rho,\theta) = \mathcal{F}^{-1}\{I_f(\rho,\theta)\}$ where $\mathcal{F}\{\cdot\}$ indicates the Fourier transform. So far the form and roundness have been separated; now the inverse discrete Radon transform of the filtered sinogram $\hat{I}(x,y) = \mathfrak{R}^{-1}\{I_f(\rho,\theta)\}$ is carried out to measure the degree of roundness in the space. If the form is represented by the image $\hat{I}(x,y)$, then $I_d = |I(x,y) - \hat{I}(x,y)|$ will be the particle's roundness. The binary image I_d will be composed of regions that correspond to the angular characteristics of the particle. The procedure is illustrated in Figure 5.

Figure 5. Procedure of the proposed algorithm. (A) Sinogram of the image (C). (B) Sinogram processed by a Butterworth filter. (C) Image of angular particle. (D) Image results of inverse Radon transform of (B). (E) Image results of subtraction of image (C) and (D); the regions correspond to the angularity of the particle. (F) Color visualization of the differences between images (C) and (D).

As mentioned above, two parameters are used for clast classification; the number of topologically unconnected regions and the percentage difference, which is defined as

$$\varepsilon = \frac{|I(x,y) - \hat{I}(x,y)|}{I(x,y)} \times 100. \qquad \text{Eq. 6}$$

The percentage difference is estimated using a cutoff frequency with $D_0 = 5$ and $n = 8$. The well-rounded, rounded and sub-rounded classes are well classified by this parameter. However, the angular and sub-angular classes cannot be differentiated with this cutoff frequency or with the percentage difference. Therefore, another filter whose cutoff frequency is determined by $D_0 = 14$ and $n = 6$ is used. For angular and sub-angular rocks, the parameter used is the number of non-overlapping regions $Np > 12$ pixels in the image I_d, which is related to the corners and curvature. Then the algorithm uses two cutoff frequencies and two parameters to classify the five roundness classes. The determination of both cutoff frequencies and the parameters is discussed in the Results and Discussion section.

3. RadonS Software

The roundness classification algorithm proposed here can be executed by the RadonS software. RadonS was programmed on the graphical user interface (GUI) of MATLAB. The software is stand-alone and was developed to work under the Windows platform. The graphic interface enables the proposed method to be used without any need for expertise in the Radon transform.

3.1 Graphical User Interface

The software has a menu bar that contains the tabs File, Radon, Export, and Help. The File menu is used to select the image. The Radon menu contains five functions: Apply, Classify, Set up filters, Set up models and Plot models. The *Apply* function executes the Radon transform algorithm described in Section 2.1, Roundness Classification Method. This function shows an image that corresponds to the differences between the original and the processed image. This image highlights the regions corresponding to roundness with color as shown in Figure 5F. The unconnected regions and the percentage difference are also estimated in this function. The *Classify* function labels each particle with one of the roundness classes. Assignment to a class is determined based on Gaussian models. The *Set Up Filters* function enables the cutoff frequencies to be set. The default cutoff frequencies are those reported in this work. Similarly, the *Set Up Models* function can change the parameters of the Gaussian models mixture. The default parameters of the Gaussian models are those reported in this work. The GMM distributions can be displayed through the *Plot Models* functions. The Export menu has two functions: *Data* and *Images*. The *Data* function creates a table with the regions found, percentage difference and the classification. These data are exported as a spreadsheet file. The *Images* function saves the images generated by the *Apply* function, which are easy and quick to interpret. Finally, the *Help* menu contains the user manual where all functions are described in detail.

3.2 Data input

The input is an image or images in jpg, tiff, bmp or png format. The image should be binary (with the particles in white and background in black), otherwise the software will segment using Otsu's method. If the image requires a robust segmentation, we suggest using ImageS or OPTGRAN-CS software. Those software were developed by our laboratory and can be freely downloaded from the public repository (https://github.com/Gamalielmch/ImageS) (Moreno et al., 2015). The image to be analyzed may contain a large number of particles. It is recommended that each particle have an area of at least 4700 pixels. RadonS software can process multiple images automatically.

3.3 RadonS software design

The software was designed in such a way that the code is as reusable as possible. View objects, control functions and variables are separated into blocks so that adding or removing any feature is easy. These blocks communicate with each other as shown in the diagram in Figure 6. The view objects are the menu bar and user interface controls (UIC). UIC are all objects that are not in the menu bar. The view objects are programmatically defined in the *RadonS_OpeningFcn* function found in the main GUI file (*RadonS.m*). In the function, it can add or remove visual elements such as buttons, text, or axes. Visual objects call control functions sharing information through the variable block. The variables are initialized and organized in a handle by the external function *variable_initialization.m*. A designer can add or remove variables by editing this function. The user can only modify the variables that the GUI allows.

Figure 6. RadonS software architecture diagram

The control block has a hierarchical flow. The user is forced to follow the order by enable/disable menu options. The user executes the control functions through the menu bar which was described in Section 1.1.1, Graphical User Interface. This block uses functions developed by us and functions of the MATLAB Image Processing Toolbox. The functions developed by us (external functions) are in separate files from the GUI. External functions can be modified for a new requirement without modifying other files. For example, the open binary images control calls an external function (*image_segmentation.m*) to segment the image, thus ensuring it is binary. This function uses the Otsu method, however the method can be changed (directly in the *image_segmentation.m* file) without modifying the software in general. This makes the code more reusable. The same is true of the *area_normalization.m*, *filtering.m*, *Radon_transform.m*, *inverse_Radon_transform.m* and, *differences_image.m* functions. In contrast, the functions to export the results (*Data* and *Images*) are within the main GUI file, so modifying them would imply a redesign of the GUI.

4. Results and discussion

In this section, the proposed algorithm is tested using the RTP reference clasts. Also, the Gaussian models used to classify the RTP reference particles are detailed. We report the results obtained by increasing the number of clasts per class, which were visually classified by a group of experts using the RTP chart. The comparison between the classifications carried out by the experts and by the algorithm is shown. Finally, we give a brief description of the Radon Software structure.

4.1 Results of the proposed algorithm

In order to test the proposed algorithm, the roundness comparison charts proposed by Russell, Taylor and Pettijohn (Müller, 1967) were used (Figure 7). The RTP reference figure consists of 25 particles organized into five different roundness categories; angular, sub-angular, sub-rounded, rounded and well-rounded.

Figure 7. Russell, Taylor and Pettijohn (Müller, 1967) comparison charts divided into five roundness categories. The particles are organized in rows, in which particles in a row belong to the same roundness classes, from top (angular) to bottom (well-rounded).

The procedure described in Section 2.1, Roundness Classification, was applied to each particle of the image shown in Figure 7. Following the algorithm, the clast area is normalized, then the sinogram is obtained by applying the Radon transform. The two-dimensional Fourier transform of the sinogram is calculated. As the sinogram's spectrum is analyzed, the magnitude of the middle frequency increases according to the degree of angularity of the particles. If the cut-off frequency is too high, the attenuation of the angled regions will be zero or almost zero and there will be no meaningful difference between the original image and the filtered image. If the cut-off frequency is too low, it will attenuate all the angular regions, even those of the rounded and sub-rounded classes, so it will not be possible to distinguish them. To find the appropriate cut-off frequencies, the distance and order were determined by an exhaustive search that maximized the distance between the classes and minimized the intra-class variance. The distance and order found for the Butterworth filter were $D_0 = 5$ and $n = 8$ for the well-rounded, rounded and sub-rounded classes and $D_0 = 14$ and $n = 6$ for the angular and sub-angular classes. The result of the lowest cut-off frequency filter is used to measure the percentage difference and the result with the highest cut-off frequency to calculate the number of non-overlapping regions. Figure 8 shows the percentage difference and number of regions found for the RTP chart.

Figure 8. Number of regions and percentage difference in I_d of the clasts shown in Figure 7.

Figure 8 shows that the classes are separated by the percentage difference and number of regions found by the two filters. In order to determine the limits of each class, we fitted bivariate Gaussian models using the mean and covariance. The mean and covariance of each class are reported in Table 1. Figure 9a shows the Gaussian models and Figure 9b the contour of the models and responses of the clasts to the filters. These Gaussian distributions can be used to determine a particle's degree of belonging to one of the classes. In fact, these models are used by the RadonS software to classify the analyzed particles.

Figure 9. (a) Bivariate Gaussian models and (b) RTP reference clast result and contour of the Gaussian models.

In order to test the algorithm, a classification made by five human experts was compared with the classification made by the proposed algorithm. The experts carried out a semi-quantitative classification of real clastic rocks based on Figure 7. There is a human bias in the classification; Moreno et al. (2015), performing a similar visual semi-quantitative analysis, found that measurement variability between different operators is around 10%. However, the increase in sample size decreases statistical uncertainty and therefore improves the models. In order to increase the number of clasts in each of the RTP roundness classes, ten more particles were added to each roundness class. They were chosen by the five experts for comparison with the RTP silhouettes from a large set of natural particles. This increased the number of particles in each roundness class to fifteen. The whole set of clasts is of volcaniclastic particles of different natures, from primary pyroclastic deposits (pyroclastic falls, flows and surges) to reworked epiclastic particles (lahar and avalanche deposits). All these particles, whether lithic or pumice, have an andesitic composition and belong to the −3 phi granulometric class. All samples come from volcanoes of the trans-Mexican volcanic belt (Colima Volcano, Nevado de Colima, and Popocatépetl). Figures A1 to A5 of the supplementary material show these 15 particles. The algorithm was applied to the new images, with the result shown in Figure 10a. The Gaussian models calculated under this condition are shown in Figure 10b. The mean and covariance of these models are reported in Table 1. The proposed algorithm classified 46 of the 50 rocks (92%) in the same class as the group of experts. Of the clasts classified in different classes, 1 was in the sub-angular class, 2 in the sub-rounded class, and 1 in the rounded class.

Figure 10. (a) Graph obtained using extended sample. (b) Contours of Gaussian models calculated using the extended sample.

Table 1. Mean and covariance of Gaussian models

Class	Parameters for 5 particles					Parameters for 15 particles				
	μ_{σ_1}	μ_{σ_2}	$\Sigma^2_{\sigma_1}$	$\Sigma^2_{\sigma_2}$	$\Sigma_{\sigma_1\sigma_2}$	μ_{σ_1}	μ_{σ_2}	$\Sigma^2_{\sigma_1}$	$\Sigma^2_{\sigma_2}$	$\Sigma_{\sigma_1\sigma_2}$
Angular	7.05	29.60	0.30	58.79	0.51	6.96	29.06	1.66	29.78	−1.22
Sub-angular	8.07	16.80	2.05	9.70	2.80	6.74	16.20	2.32	10.02	2.27
Sub-rounded	5.35	4.80	2.55	5.70	2.42	4.36	5.86	2.57	8.55	−0.78
Rounded	2.64	1.00	0.10	1.50	-0.14	2.63	1.33	0.25	0.80	−0.13
Well-rounded	0.45	2.8e−1	0.42	2e−11	2.3e−6	0.31	0	0.17	5e−11	8e−7

It should be noted that the proposed method is designed to classify contours; that is, it analyzes two-dimensional functions. Sedimentary rock shape analysis is a three-dimensional problem, so the proposed method faces the same limitations as methods that use a single image.

5. Conclusions

A method and software based on the Radon transform was proposed to classify the roundness of sedimentary rocks. The image sinogram contains information on the roundness of the clast. This work shows that the difference between the original image and the image obtained from the filtered sinogram produces regions that are related to the different degrees of roundness. Using the response from two filters, the number of non-superimposed regions, and percentage difference, it is possible to classify clasts into five classes as proposed by Russell, Taylor and Pettijohn. The algorithm was tested with the chart of Russell, Taylor and Pettijohn and by a classification performed by a group of experts. The proposed algorithm classified 94% of the rocks of a sample of 75 clasts in the same categories as the experts.

Moreover, using the number of non-superimposed regions and percentage difference, we have determined Gaussian models that enable the analyzed clasts to be assigned to specific roundness classes. We provide two different model parameters, one using the 25 reference clasts of Russell, Taylor and Pettijohn, and the other adding the 50 sample clasts classified by the experts.

In order to facilitate the use and promote the diffusion of the algorithm in the geological science community, we developed software with a graphical interface on the MATLAB platform. The RadonS software can be freely downloaded from the public repository https://github.com/Gamalielmch/RadonS.

Acknowledgment

We acknowledge the Consejo Nacional de Ciencia y Tecnología (CONACYT) for partial support of this work and for the *Retención* grant (No. 2019-000010-01NACV-00020) of Dr. Gamaliel Moreno. We also acknowledge Dr. Luis Ángel Sedano, Ilze Sanchez and Maria Fernanda Cerca for their support in the classification.

References

Alshibli, K. A., Mustafa, I. A., 2004. Characterizing Surface Roughness and Shape of Sands Using Digital Microscopy. Journal of Computing in Civil Engineering 18 (1),36-45. https://doi.org/10.1061/(ASCE)0887-3801(2004)18:1(36)

Barrett, H. H., 1984. III The Radon Transform and Its Applications. Progress in Optics, edited by E. Wolf, USA, Vol 21, 217-286. Elsevier. https://doi.org/10.1016/S0079-6638(08)70123-9

Barrett, P. J., 1980. The Shape of Rock Particles, a Critical-Review. Journal Sedimentology 27 (3), 291-303. https://doi.org/10.1111/j.1365-3091.1980.tb01179.x

Beddow, J. K., 2018. Particle Characterization in Technology: Volume II: Morphological Analysis, 1st Edn. CRC Series on Fine Particle Science and Technology, Florida, USA, 288pp.

Blott, S. J., Pye, K., 2008. Particle shape: a review and new methods of characterization and classification. Sedimentology 55 (1), 31-63. https://doi.org/10.1111/j.1365-3091.2007.00892.x

Boggs, Jr. Sam. 2012. Petrology of sedimentary rocks. 2nd Edn. Cambridge university press, New York, USA, 600pp. https://doi.org/10.1017/CBO9780511626487

Caballero, L., Sarocchi, D., Borselli, L.,Cárdenas, A. I., 2012. Particle interaction inside debris flows: Evidence through experimental data and quantitative clast shape analysis. Journal of Volcanology and Geothermal Research 231-232, 12-23. https://doi.org/10.1016/j.jvolgeores.2012.04.007

Charpentier, I. , Sarocchi, D., Rodriguez, L. A., 2013. Particle shape analysis of volcanic clast samples with the Matlab tool MORPHEO. Computers & Geosciences 51, 172-181. https://doi.org/10.1016/j.cageo.2012.07.015

Deans, S.R., 1983. The Radon Transform and Some of Its Applications. 1st edn, John Wiley & Sons Inc., New York, USA.

Diepenbroek, M., Bartholomä, A., Ibbeken, H., 1992. How round is round? A new approach to the topic 'roundness' by Fourier grain shape analysis. Sedimentology 39 (3), 411-422. https://doi.org/10.1111/j.1365-3091.1992.tb02125.x

Douglas, I. B., Colin, K. B., 1993. The description and representation of particle shape. Earth Surface Processes and Landforms 18 (7), 665-672. https://doi.org/10.1002/esp.3290180709

Ehrlich, R., Weinberg, B., 1970. An exact method for characterization of grain shape. Journal of Sedimentary Research 40 (1), 205-212. https://doi.org/10.1306/74D71F1E-2B21-11D7-8648000102C1865D

Folk, R. L., 1980. Petrology of sedimentary rocks. 1st Edn, Hemphill Publishing Company, Texas, USA, 182pp.

Helgason, S., 1999. The Radon Transform, 2nd edn. Progress in Mathematics, Vol 5., Massachusetts, USA, https://doi.org/10.1007/978-1-4757-1463-0

Hryciw, R.D, Zheng, J., Shelter, K., 2016. Particle roundness and sphericity from images of assemblies by chart estimates and computer methods. Journal of Geotechnical and Geoenvironmental Engineering 142 (9), 04016038. https://doi.org/10.1061/(ASCE)GT.1943-5606.0001485

Kaye, B. H., 1978. Specification of the ruggedness and/or texture of a fine particle profile by its fractal dimension. Powder Technology 21 (1), 1-16. doi: https://doi.org/10.1016/0032-5910(78)80103-X

Kelley, B. T., Madisetti, V. K., 1993. The fast discrete Radon transform. I. Theory. IEEE Transactions on Image Processing 2 (3), 382-400. https://doi.org/10.1109/83.236530

Krumbein, W. C., Pettijohn, F.I., 1938. Manual of Sedimentary Petrography. 1st Edn, Appleton-Century-Crofts, Inc., New York, USA, 549 pp.

Krumbein, W. C. 1941. Measurement and Geological Significance of Shape and Roundness of Sedimentary Particles. SEPM Journal of Sedimentary Research Vol. 11 (2), 64-72. https://doi.org/10.1306/d42690f3-2b26-11d7-8648000102c1865d

Kuchment, P., 2014. The Radon Transform and Medical Imaging. Society for Industrial and Applied Mathematics, Philadelphia, Pennsylvania, U.S. 233p. https://doi.org/10.1137/1.9781611973297

Leavers, V. F., 2000. Use of the two-dimensional Radon transform to generate a taxonomy of shape for the characterization of abrasive powder particles. IEEE Transactions on Pattern Analysis and Machine Intelligence 22 (12), 1411-1423. https://doi.org/10.1109/34.895975

Montenegro R. A., Sarocchi, D., Nahmad M. Y., Borselli, L., 2013. Form From Projected Shadow (FFPS): An algorithm for 3D shape analysis of sedimentary particles. Computers & Geosciences 60, 98-108. https://doi.org/10.1016/j.cageo.2013.07.008

Moreno, G., Sarocchi, D., Santana E. A., Borselli, L., 2015. Optical granulometric analysis of sedimentary deposits by color segmentation-based software: OPTGRAN-CS. Computers & Geosciences 85, 248-257. https://doi.org/10.1016/j.cageo.2015.09.007

Müller, G., 1967. Methods in Sedimentary Petrology. Hafner Publishing Co., New York 183 pp.

Orford, J. D.,Whalley, W. B., 1983. The use of the fractal dimension to quantify the morphology of irregular-shaped particles. Sedimentology 30 (5), 655-668. https://doi.org/10.1111/j.1365-3091.1983.tb00700.x

Powers, M. C., 1953. A New Roundness Scale for Sedimentary Particles. SEPM Journal of Sedimentary Research Vol. 23 (2), 117-119. https://doi.org/10.1306/d4269567-2b26-11d7-8648000102c1865d

Powers, M. C., 1982. Comparison chart for estimating roundness and sphericity. AGI data sheet 18 (1).

Radon, J., 2005. On the determination of functions from their integral values along certain manifolds. IEEE Transactions on Medical Imaging, vol. 5, no. 4, pp. 170-176, Dec. 1986. https://doi.org/10.1109/TMI.1986.4307775

Roussillon, T., Piégay, H., Sivignon, I., Tougne, L., Lavigne, F., 2009. Automatic computation of pebble roundness using digital imagery and discrete geometry. Computers & Geosciences 35 (10), 1992-2000. https://doi.org/10.1016/j.cageo.2009.01.013

Sarocchi, D., Borselli, L., Macías, J.L., 2008. New tools to investigate textures of pyroclastic deposits. IOP Conference Series: Earth and Environmental Science 3 (1), 012009. https://doi.org/10.1088%2F1755-1307%2F3%2F1%2F012009

Sarocchi, D., Sulpizio, R., Macías. J. L., Saucedo, R., 2011. The 17 July 1999 block-and-ash flow (BAF) at Colima Volcano: New insights on volcanic granular flows from textural analysis. Journal of Volcanology and Geothermal Research 204 (1), 40-56. https://doi.org/10.1016/j.jvolgeores.2011.04.013

Schwarcz, H. P., Shane, K. C., 1969. Measurement of Particle Shape by Fourier Analysis. Sedimentology 13 (3-4), 213-231. https://doi.org/10.1111/j.1365-3091.1969.tb00170.x.

Sneed, E. D., Folk, R.L., 1958. Pebbles in the Lower Colorado River, Texas a Study in Particle Morphogenesis. The Journal of Geology 66 (2), vol. 66, no. 2, 1958, pp. 114–150. https://doi.org/10.1086/626490

Stachowiak, G. W., 1998. Numerical characterization of wear particle morphology and angularity of particles and surfaces. Tribology International 31 (1), 139-157. https://doi.org/10.1016/S0301-679X(98)00016-4

Tabbone, S., Wendling, L., 2002. Technical symbols recognition using the two-dimensional Radon transform. Object recognition supported by user interaction for service robots, Quebec, Canada, 2002, pp. 200-203 vol.3. https://doi.org/10.1109/ICPR.2002.1047829

Tucker, M. E., 2003. Sedimentary Rocks in the Field. 3rd edn, John Wiley & Sons Ltd, Chichester, England, 234 pp.

Tucker, M. E., 2009. Sedimentary Petrology: An Introduction to the Origin of Sedimentary Rocks, 3rd edn, Blackwell Science, Durham, England, 262 pp.

Wadell, H., 1932. Volume, Shape, and Roundness of Rock Particles. The Journal of Geology, vol. 40, no. 5, pp. 443–451.

Winkelmolen, A. M. 1982. Critical remarks on grain parameters, with special emphasis on shape. Sedimentology 29 (2), 255-265. https://doi.org/10.1111/j.1365-3091.1982.tb01722.x

Zingg, T. 1935. Contribution to the gravel analysis. Schweiz Petrog. Mitt. 15, Original manuscript in German.

Appendix A.

Figures showing the clasts proposed by Russell, Taylor and Pettijohn and those classified by the experts.

Figure A1. Clast features corresponding to the angular class

Figure A2. Clast features corresponding to the sub-angular class

Figure A3. Clast features corresponding to the sub-rounded class

Figure A4. Clast features corresponding to the rounded class

Figure A5. Clast features corresponding to the well-rounded class

Computer Code Availability

We have developed a software called RadonS V1.0, which contains the code of the method and graphical interface developed by us. RadonS V1.0 is distributed under GNU General Public License version 3. The code has been programmed in MATLAB 2014b. The main file is *RadonShape.m*. This file contains multiple functions. In the *RadonShape_OpeningFcn* function, the global variables and elements of the graphic interface are declared. The *load_Callback* function loads and binarizes the image. The *Radon_Callback* function is the main function and carries out the method described in this manuscript. The *Radon_setupmodels_Callback* and *Radon_plotmodels_Callback* functions adjust and plot the means and variances of the Gaussian models respectively. The *class_Callback* function classifies the particles in the analyzed images. The functions that export the images and data are *expdata_Callback* and *expima_Callback*. The rest of the functions are related to the graphic elements of the graphic interface. In addition to the main *RadonShape.m* file, we have incorporated the *RadonShape.fig* file, which is used to modify the interface from the MATLAB GUI. The modules *area_normalization*, *assignment*, *differences_image*, *filtering*, *image_segmentation*, *inverse_Radon_transform*, *lpfilter*, *models*, *Radon_transform*, *and variable_initialization* are functions that are called by the main file.

We have put all the files necessary to test, use and edit the software in the public repository. In addition to the files mentioned above, we have incorporated a readme.txt with the general information of the manuscript and the use and general description of the code. We have also included a manual that provides detailed information about the use of the software. We have added two folders, one of them with the test images (ten images) and another one with the output files of these images.

The code used to generate the graphic interface and full source files can be downloaded from the public repository https://github.com/Gamalielmch/RadonS.

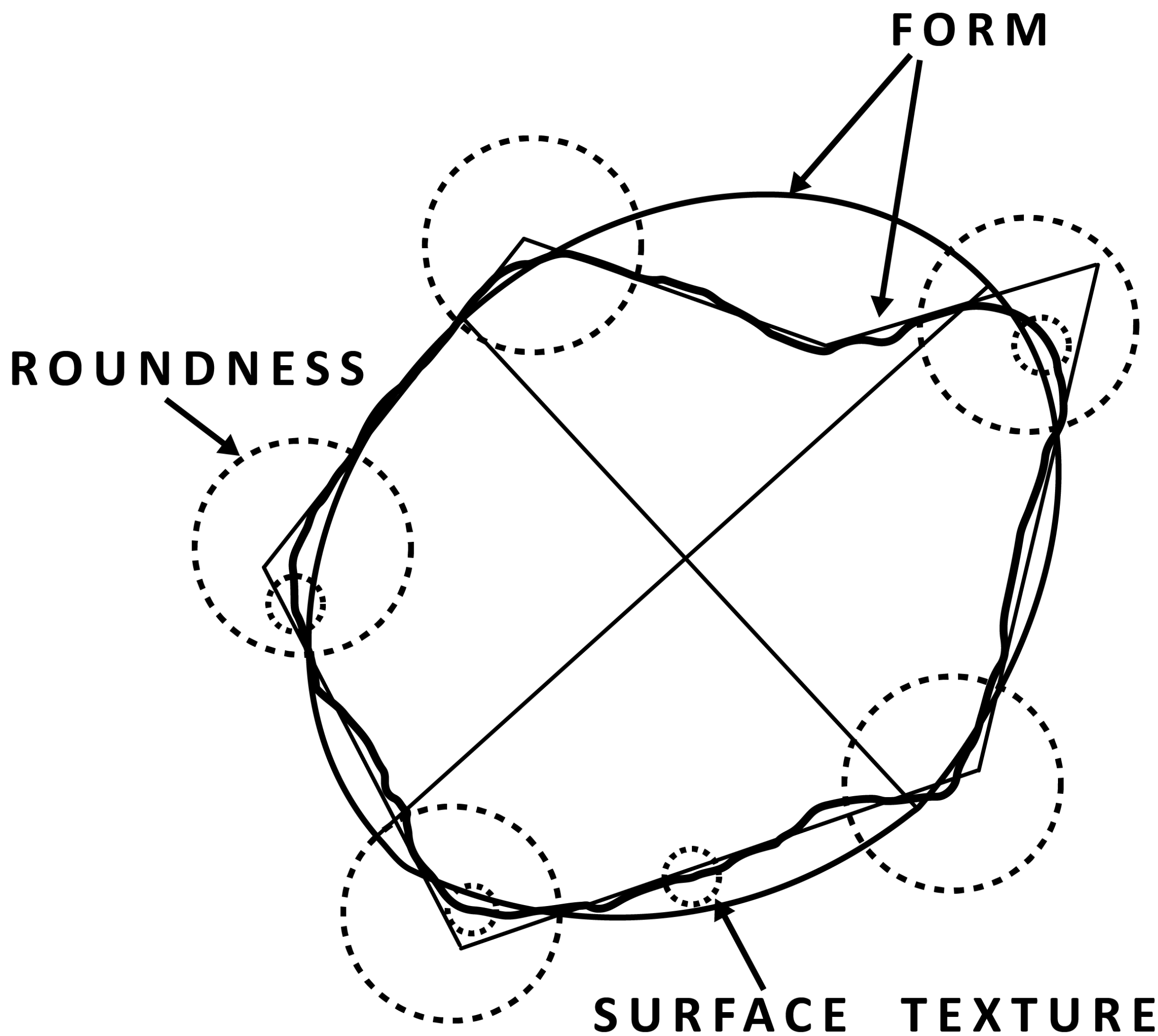
FORM
ROUNDNESS
SURFACE TEXTURE

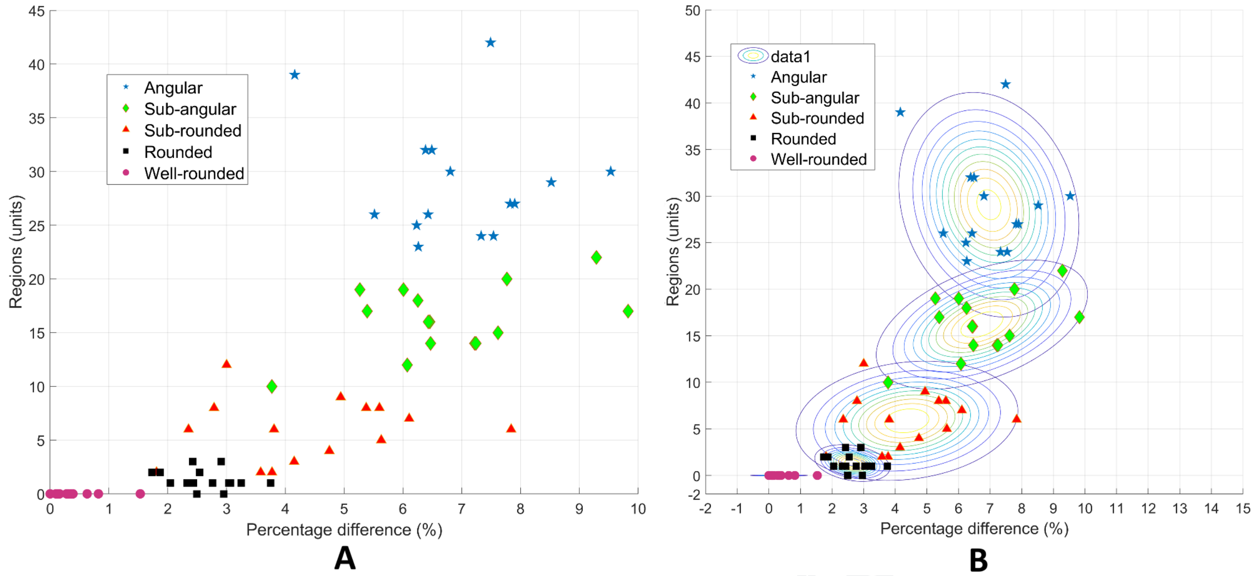

Angular
Sub-angular
Sub-rounded
Rounded
Well-rounded
Regions (units)
Percentage difference (%)
A
data1
Angular
Sub-angular
Sub-rounded
Rounded
Well-rounded
Regions (units)
Percentage difference (%)
B

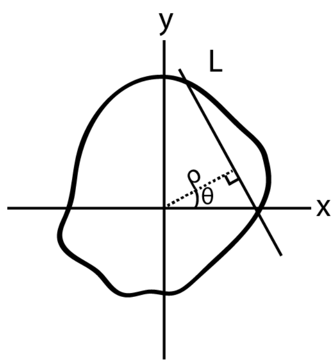

y
L
ρ
θ
x

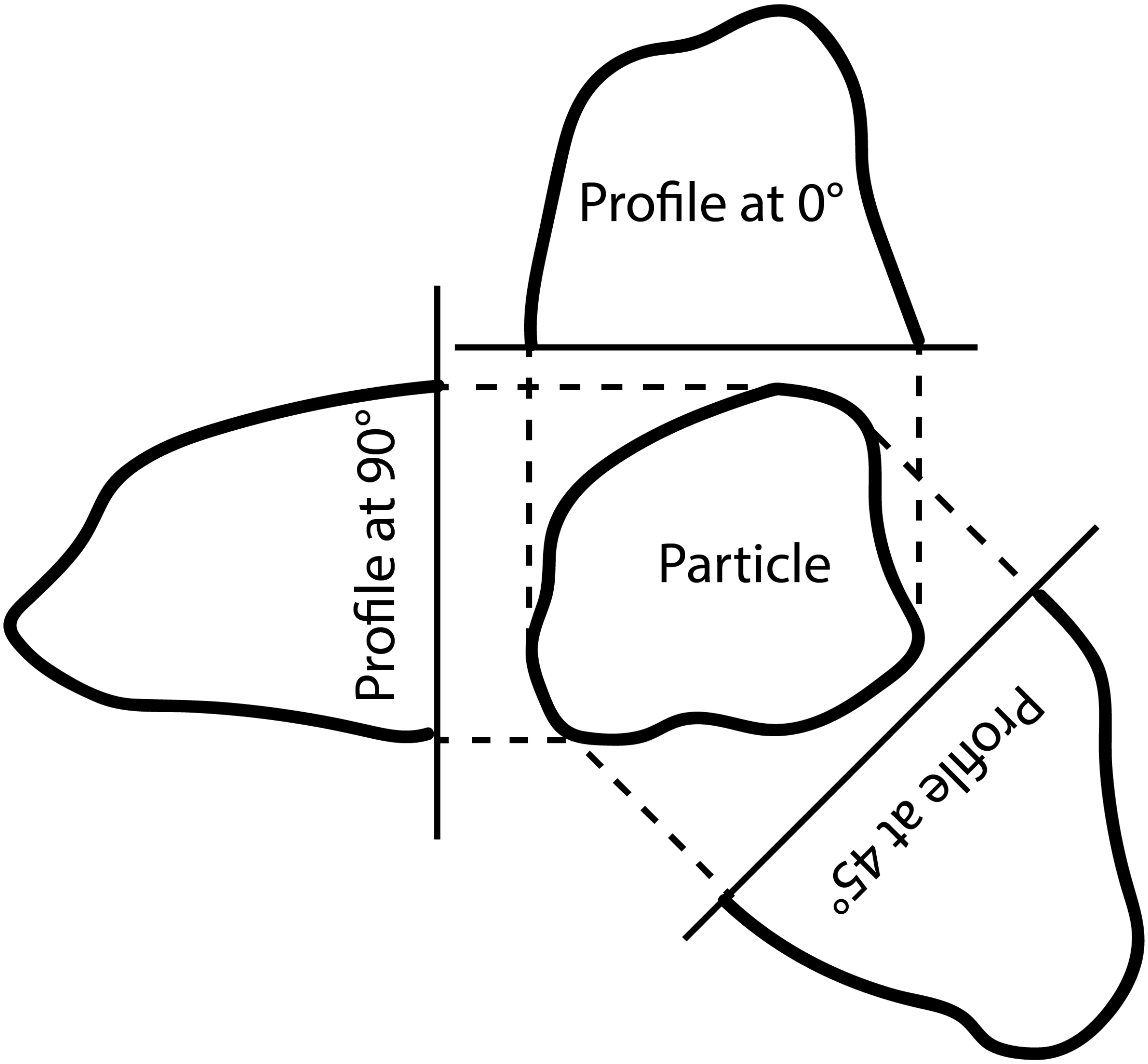
Profile at 0°
Profile at 90°
Particle
Profile at 45°

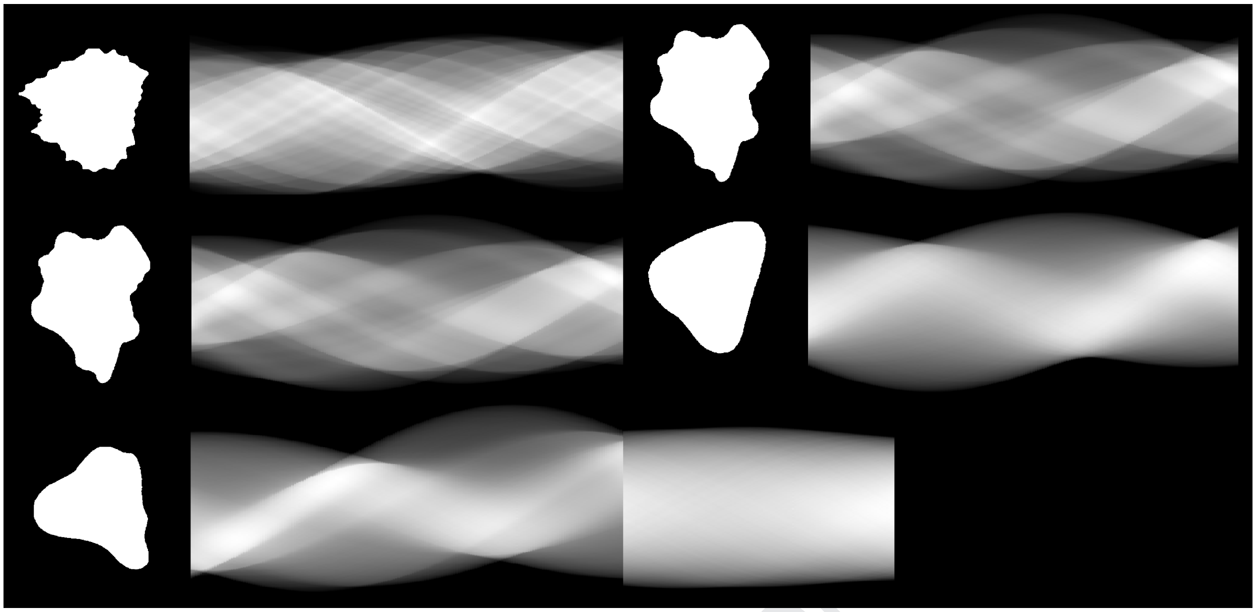

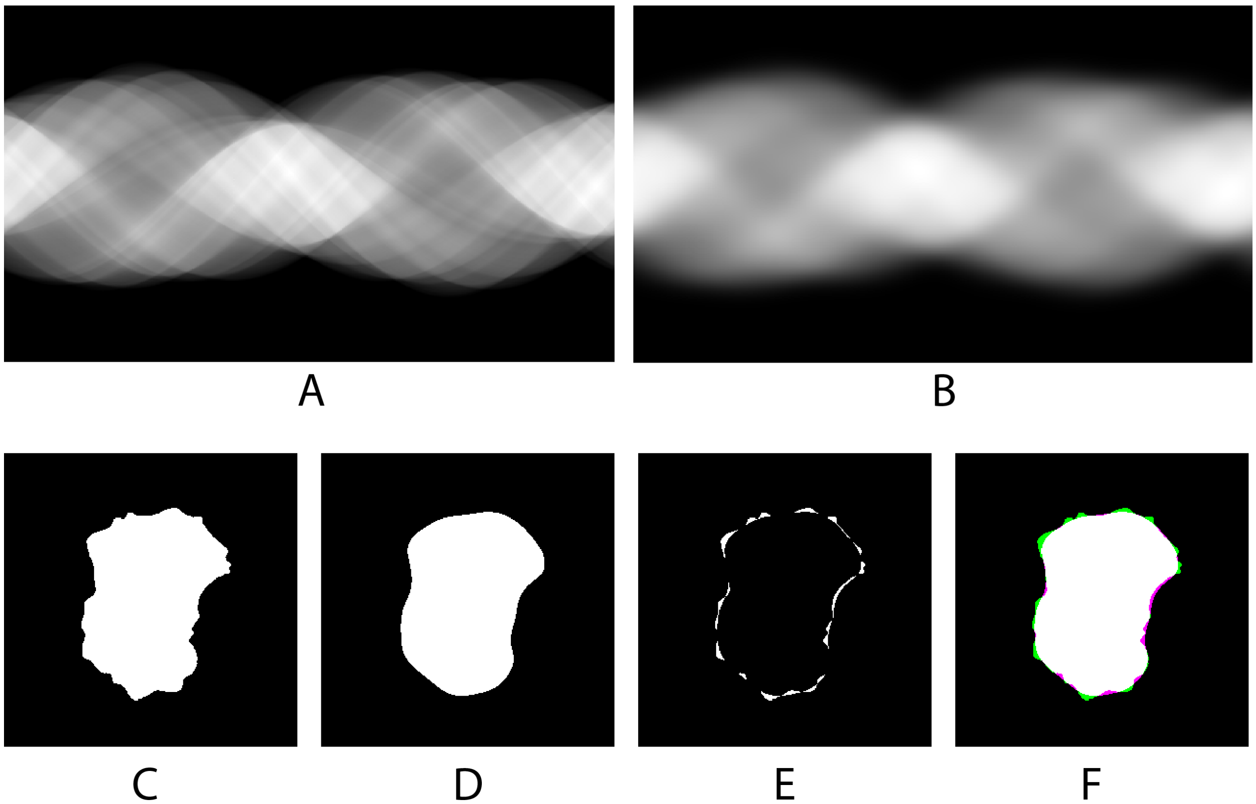
A
B
C
D
E
F

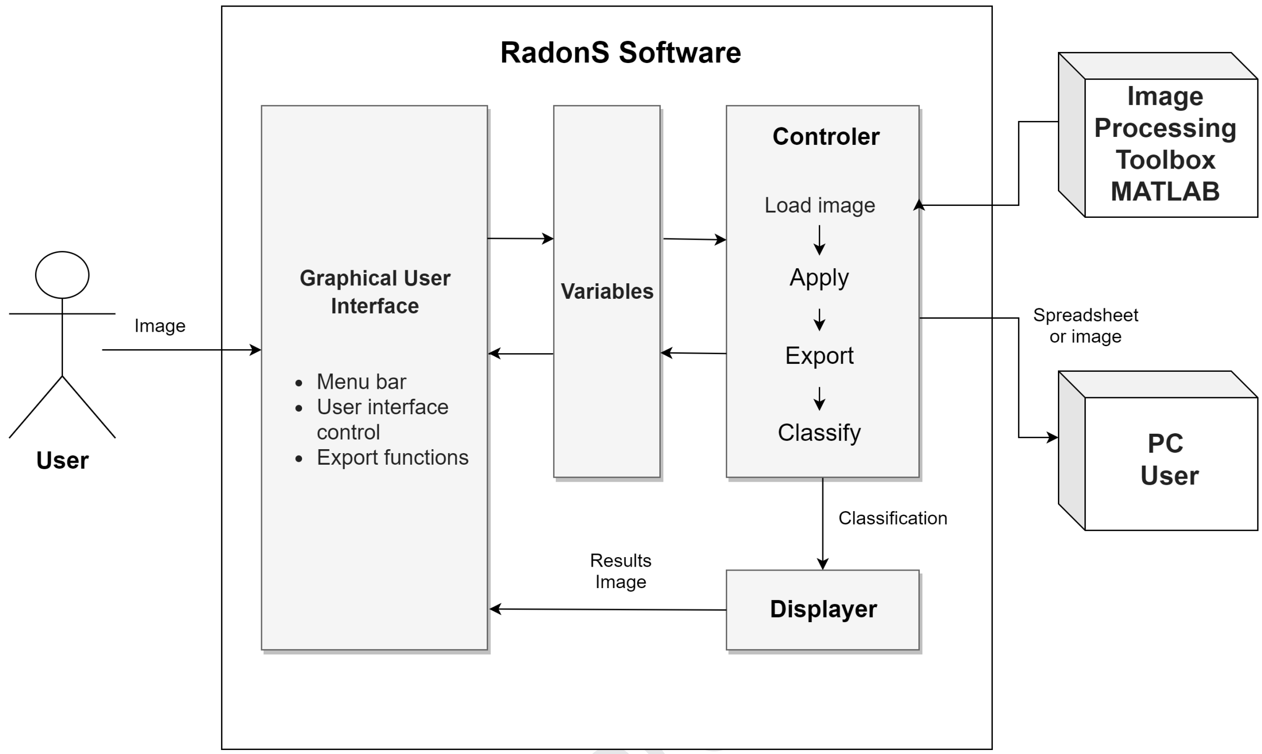
RadonS Software
Graphical User Interface
Menu bar
User interface control
Export functions
Variables
Controler
Load image
Apply
Export
Classify
Displayer
Image
User
Results Image
Classification
Image Processing Toolbox MATLAB
Spreadsheet or image
PC User

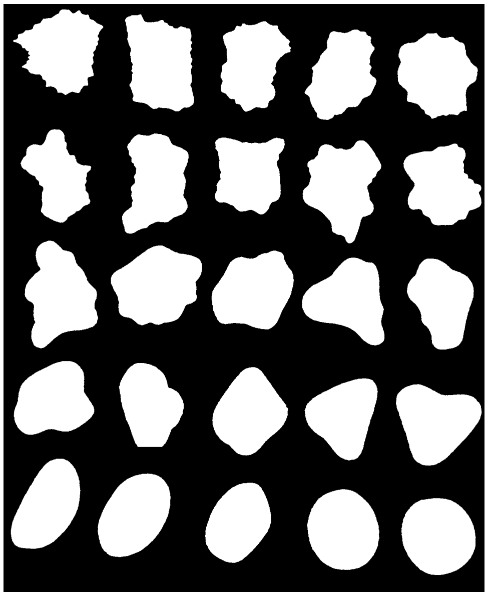

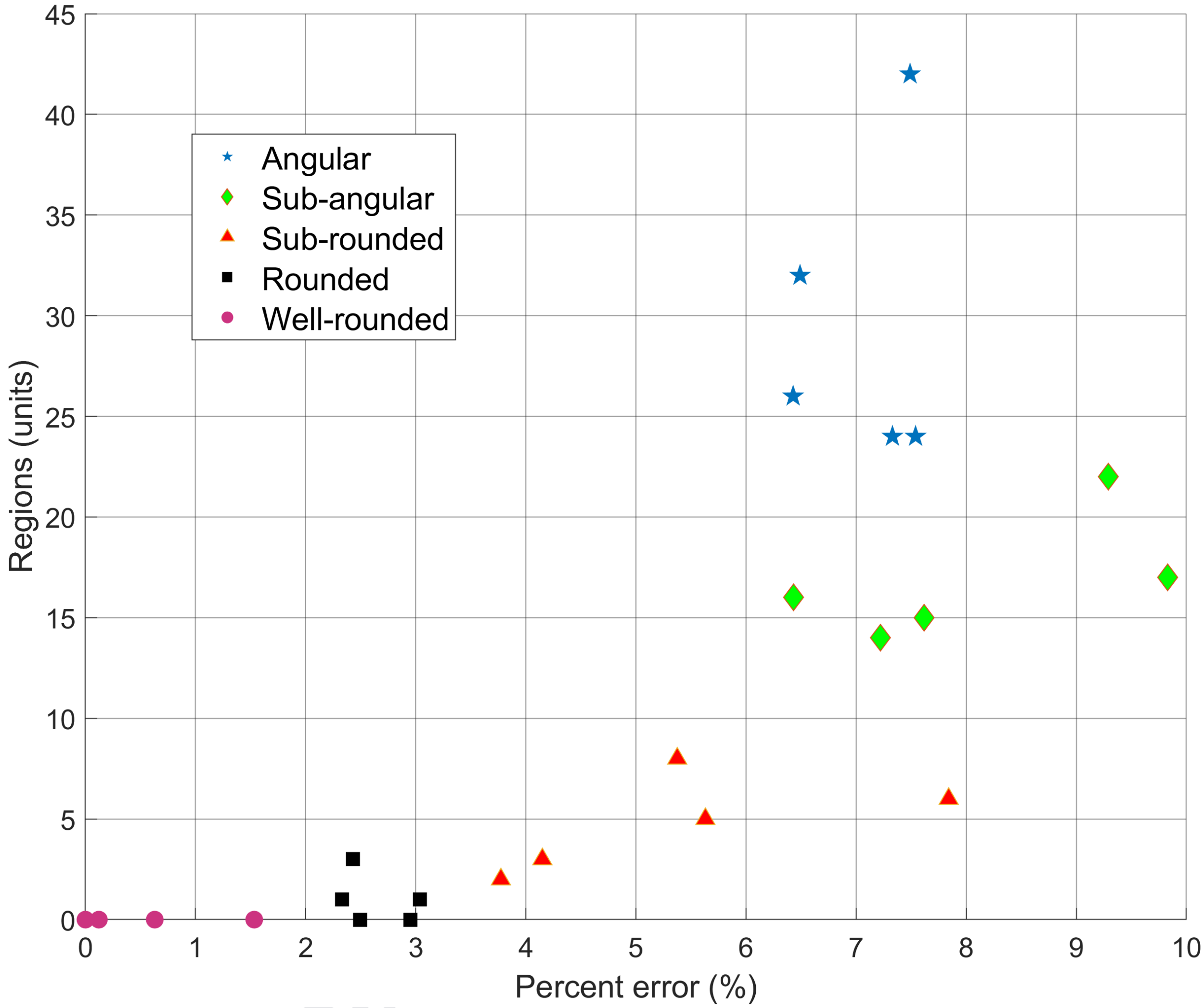
Angular
Sub-angular
Sub-rounded
Rounded
Well-rounded
Regions (units)
Percent error (%)
0
5
10
15
20
25
30
35
40
45
0
1
2
3
4
5
6
7
8
9
10

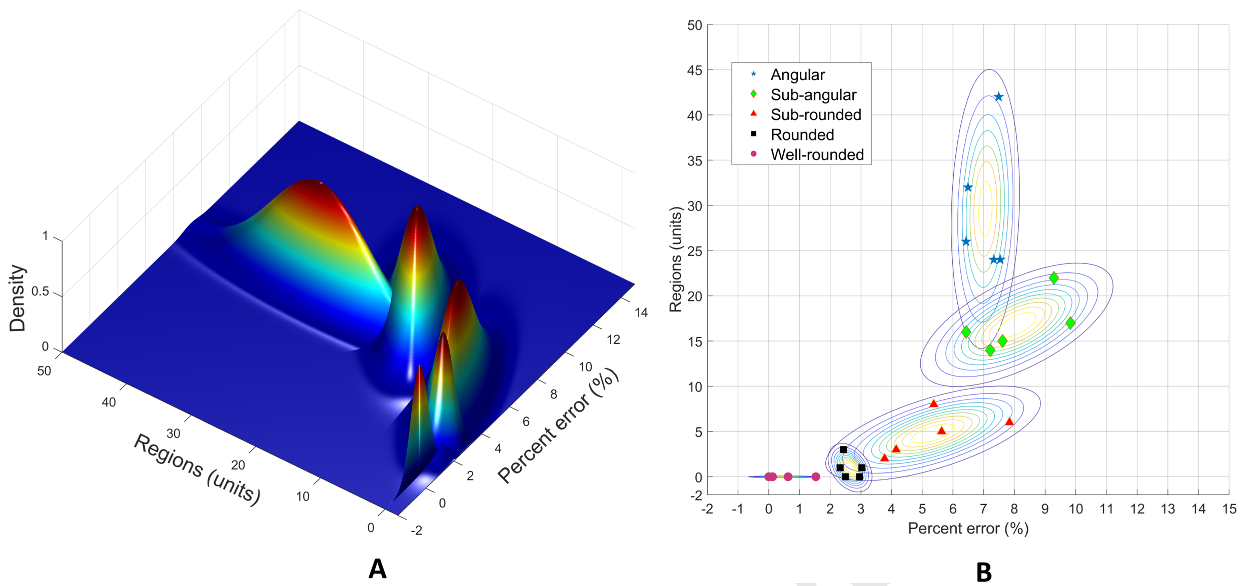

Density
Regions (units)
Percent error (%)
A
Angular
Sub-angular
Sub-rounded
Rounded
Well-rounded
Regions (units)
Percent error (%)
B

We developed a method for classifying clast roundness based on Radon transform

The sinogram is filtered and subtracted from the original image in space

The percentage error and the number of unconnected regions are used to classify

The method was tested with the charts proposed by Russell, Taylor and Pettijohn

The proposed algorithm is accurate and the software is original and freeware